Depletion of mitochondrial DNA in fibroblast cultures from patients with POLG1 mutations is a consequence of catalytic mutations

Neil Ashley[1], Anthony O'Rourke[2], Conrad Smith[2], Susan Adams[2], Vasantha Gowda[1], Massimo Zeviani[3], Garry K. Brown[4], Carl Fratter[2] and Joanna Poulton[1,*]

[1]Nuffield Department of Obstetrics and Gynaecology, University of Oxford, The Women's Centre, John Radcliffe Hospital, Oxford OX3 9DU, UK, [2]Oxford Medical Genetics Lab, Churchill Hospital, Oxford, UK, [3]Division of Molecular Neurogenetics, National Neurological Institute 'C. Besta', Milano 20126, Italy and [4]Department of Biochemistry, University of Oxford, Oxford, UK

We investigated clinical and cellular phenotypes of 24 children with mutations in the catalytic (alpha) subunit of the mitochondrial DNA (mtDNA) gamma polymerase (POLG1). Twenty-one had Alpers syndrome, the commonest severe POLG1 autosomal recessive phenotype, comprising hepatoencephalopathy and often mtDNA depletion. The cellular mtDNA content reflected the genotype more closely than did clinical features. Patients with tissue depletion of mtDNA all had at least one allele with either a missense mutation in a catalytic domain or a nonsense mutation. Four out of 12 patients exhibited a progressive, mosaic pattern of mtDNA depletion in cultured fibroblasts. All these patients had mutations in a catalytic domain in both POLG1 alleles, in either the polymerase or exonuclease domain or both. The tissue mtDNA content of patients who had two linker mutations was normal, and their phenotypes the mildest. Epilepsy and/or movement disorder were major features in all 21. Previous studies have implicated replication stalling as a mechanism for mtDNA depletion. The mosaic cellular depletion that we have demonstrated in cell cultures may be a manifestation of severe replication stalling. One patient with a severe cellular and clinical phenotype was a compound heterozygote with POLG1 mutations in the polymerase and exonuclease domain in*trans*. This suggests that POLG1 requires both polymerase and 3′–5′ exonuclease activity in the same molecule. This is consistent with current functional models for eukaryotic DNA polymerases, which alternate between polymerizing and editing modes, as determined by competition between these two active sites for the 3′ end of the DNA.

INTRODUCTION

First described in 1991, mtDNA depletion is the central feature of a group of disorders, collectively termed mtDNA depletion syndromes (MDS) (1,2). The characteristic mtDNA finding in these disorders is a quantitative reduction in the mtDNA content of affected tissues, but there may also be low levels of heteroplasmy for point mutations (3). Defects in mtDNA maintenance have been hard to study as the mtDNA defects are only evident in primary fibroblast cultures (4) from a minority of patients and are rarely

described in other primary lines (5). Unlike mtDNA mutations, the pattern of inheritance of MDS is autosomal recessive. Furthermore, mtDNA content and OXPHOS activity was restored in cybrids generated from the fusion of mtDNA-free (ρ°) cells with enucleated fibroblasts from MDS patients (6), implying an underlying nuclear defect.

Previous investigators have classified MDS into two main groups, consisting of a hepatocerebral form and a myopathic form (7,8). In both groups several tissues may be affected (9). Genes involved in the hepatocerebral form include POLG1 (10), deoxyguanosine kinase (dGK) (11), the human

---

*To whom correspondence should be addressed. Tel: +44 1865221007; Fax: +44 1865769141; Email: joanna.poulton@obs-gyn.ox.ac.uk

ortholog of the mouse kidney disease gene MPV17 (12), the mitochondrial helicase/primase, TWINKLE (13) and the alpha subunit of Succinyl-CoA Synthase (SUCLG1) (14). MDS without hepatic involvement is associated with myopathy and/or encephalopathy. Mutations have been identified in genes encoding the mitochondrial thymidine kinase (TK2) (11), the beta subunit of ADP-Forming Succinyl-CoA Synthase (SUCLA2) (15), the P53 dependent subunit of ribonucleotide reductase (RRM2B) (16) and thymidine phosphorylase (or TP, associated with MyoNeuroGastroIntestinal Encephalomyopathy or MNGIE) (17). Myopathic MDS may present as the so-called 'benign' later-onset mtDNA depletion (18).

By far the commonest gene defects identified in autosomal recessive mtDNA depletion are POLG1 mutations. POLG1 is the gene encoding the 195 kDa catalytic (alpha) subunit of the mitochondrial (gamma) DNA polymerase, located on chromosome 15q25. Three polymerase domains (exons 17–22) are separated from 3 exonuclease domains (exons 2–8) by a linker region (residues 418–755) that interacts with the beta subunit. Mutations in POLG1 are associated with a range of different phenotypes (19). These include both dominant and recessive chronic progressive ophthalmoplegia, mitochondrial recessive ataxia syndrome (20) and recessive, severe, early onset Alpers syndrome (10). While some authors distinguish between Alpers syndrome, characterized by refractory seizures, deafness, cortical blindness, episodic psychomotor regression, and Alpers–Huttenlocher syndrome in which liver disease is also a major feature (21), such a subdivision requires detailed data. Alpers syndrome is marked by a progressive deterioration, most patients dying in infancy but a few surviving into their teens (22). POLG1 genotype:phenotype correlations in both Alpers and mtDNA depletion have been disappointing (19). We sought to develop these using accurate quantitation of tissue mtDNA content and cellular depletion phenotype.

RESULTS

We investigated 24 children in whom we had identified POLG gene mutation(s). These patients were referred with childhood onset of symptoms that were suggestive of POLG1 mutations, such as Alpers syndrome, or because we had previously identified mtDNA depletion or multiple DNA deletions. Features of the 24 patients with POLG1 mutations are summarized in Table 1. Age ranged from 0 to 17 years and 9/10 patients with mtDNA depletion in liver or muscle were male.

Genotype–phenotype correlation

Sequence analysis of the POLG1 gene revealed two mutant alleles in all of the patients with Alpers disease consistent with recessive inheritance. Three individuals had a largely neurological presentation that clearly fell outside the accepted criteria for Alpers disease, but the remainder all had encephalopathy. Seventeen out of the remaining 23 (74%) had a variable degree of liver dysfunction, from mild to liver failure requiring transplant. Of the 20 out of 21 individuals with probable Alpers syndrome where clinical information was available, all had epilepsy, which was intractable (epilepsia

partialis continua) in four. One teenage patient died only 2 years after presentation, ending with 5 months of continuous seizure activity. Epilepsy was treated with sodium valproate in four out of the 11 where we had information about anticonvulsant therapy, and in one case this was followed by deterioration and death within 3 months. Movement disorders (choreoathetosis, ataxia and ataxic nystagmus) and epilepsia partialias continua were common features. None of the patients had survived to their 19th birthday, the median age at death being 1 year (7 months to 18 years).

The mtDNA content of liver was low in all cases where it was available, but was variable in muscle (22–117%). All of the patients with mtDNA depletion in liver and/or muscle had at least one missense or nonsense mutation in a catalytic domain, either at least one mutation in the polymerase domain or two mutations in the exonuclease domain.

Fibroblast nucleoid mtDNA distribution defines a distinctive subgroup of patients with mosaic cellular depletion that is reflected by low mtDNA content of tissue and poor life expectancy

Fibroblast cultures were available for 10/24 of the patients for visualizing mtDNA using PicoGreen fluorescence microscopy. PicoGreen can quantitatively stain mtDNA (23), which *in vivo* is arranged into punctate DNA/protein structures termed nucleoids, which consist of several mtDNA genomes complexed to nucleoid proteins like POLG. In normal control cells, PicoGreen stains numerous nucleoids that are of comparable fluorescence intensity in different cells and between different individuals. However, some of the patient fibroblast cultures, such as that from patient A (Fig. 1) showed mosaic depletion, in that many cells showed greatly reduced nucleoid staining, suggesting mtDNA depletion, which was most noticeable at later cell passages (approximately 2–3 months continuous culture). This was evident in cultured cells derived from four individuals (patients A–D Fig. 1 and Table 1). In all cases nuclear staining was unaffected, although cytoplasmic background fluorescence was often increased. These patients with mosaic depletion within their cultured fibroblasts all had severe clinical phenotypes, all being dead by the age of 16 months. Of these, patient A had much the highest proportion of depleted cells, and this was probably a later passage than cultures B–D. The mosaic distribution of mtDNA depletion was also apparent at low cell passage number (Supplementary Material, Fig. S1), where occasional mtDNA-free (rho zero) cells were present (Supplementary Material, Fig. S1), interspersed with cells with apparently normal or near normal mtDNA levels. Cultures A–C were grown until at least passage 20, and the proportion of depleted cells increased with successive passage (compare Fig. 1 with Supplementary Material, Fig. S1), so that by 45 days the majority of cells were depleted (Fig. 2A). This was reflected by a reduced minimum fibroblast mtDNA content by Q-PCR (Table 1) in cells from patients A–D (average 23%), but at baseline patient D had infrequent depleted cells and much higher mtDNA content (97%, relative to control fibroblast cultures 39–193%). There was no consistent change in mtDNA content in any of the fibroblast cultures from controls (Fig. 2), from patients with other types of mitochondrial

Table 1. Patient phenotypes

Identifier	Sex	Mutation	Mutation Location	Cellular Depletion?	Age Onset	mtDNA content (%)				Epilepsy	Hepatopathy	Movement disorder
						Liver	Muscle	Fibroblasts	Valproate			
A (22,27)	M	T914*P*+R1096C	P+P	Yes	<1 year	7	23	19–27		+	+	(+)
B	M	H277C+ T851A	P+E	Yes	6 months	4	32	36–60		+	+	
C	M	R1096C homozygous	P+P	Yes	5 months			16–55		+	+	
D (38)	F	R232G+[T251I;P587L]	E+[EL]	Yes	5 months	4		22–97		+	+	
E (29)	M	R627W+T914P	P+L	Borderline	Birth	5	54	30–77	−	+	+	+
F	M	W748S+[R852C;G11D]	P+L	No	1 year	32		38	+	+	+	(+)
G	M	A467T+[R852C;G11D]	P+L	No	2 years 3 months		22	37	−	+	+	−
H	F	A467T+T914P	P+L	No	7 months		39	62		+	+	+
I	M	W748S+T914P	P+L	No	4 years	15		84	+	+	+	+
J (21,27)	M	E873X+ A467T	L+X	Borderline	18 months	25	30	51		+	+	+
K	M	A467T+W347_L365del	E+L	Unknown	7 months				−	+	+	(+)
L	F	W748S+W748S	L+L	Unknown	16 years		108		+	+	(+)	(+)
M	F	L304R homozyg	E+E	Unknown	10 year		117		−	−	−	−
N	M	W748S+T914P	P+L	Unknown	13 months		43			+	+	+
O	F	W748S+G848S	P+L	Unknown	6 years	−	−	−		+	−	+
P	F	A467T+T914P	P+L	Unknown	15 years	−	−	−			+	
Q	F	A467T+G848S	P+L	Unknown	18 months				−	+	(+)	−
R	F	A467T+L966R	P+L	Unknown	4 years					+		−
S	F	A467T+R374X	L+X	Unknown	4 months				−	+	+	(+)
T	M	A467T+R417T	E+L	Unknown	2 years	−	−	−			−	
U	M	H569Q homozygous	L+L	Unknown	15 years		78			−	−	
V	M	W748S+[P587L,P589L]	L+L	Unknown	17 years	−	−	−		+	−	
W	F	A467T+A467T	L+L	Unknown	16 years	−	−	−		+		+
X	F	A467T+C418R	L+L	Unknown	3 years	−	−	−		+	−	+
Mean (%)						13.1	54.6					
Controls						40–152	60–140	39–193				

P, mutation in polymerase domain; P+P, two mutations in polymerase domain; L, Linker domain; E, exonuclease domain; X, nonsense mutation.
Blanks denote unknown; +, present; (+); present but not prominent; −, absent.
Fibroblast mtDNA content were measured on several occasions on the lines containing rho zero cells, range shown.
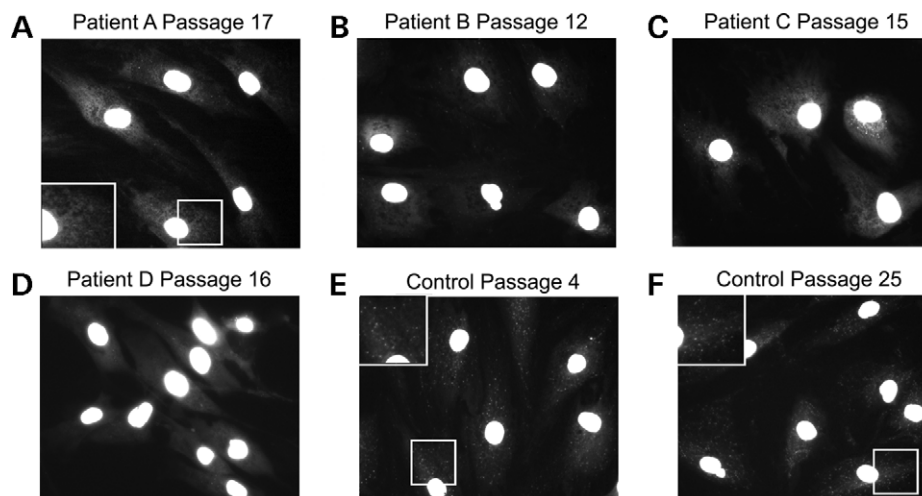
Figure 1. PicoGreen staining reveals marked mtDNA depletion in certain MDS patient derived fibroblast cell cultures, that alters with cell passage (**A**) Pico-Green staining of a later passage of patient A's cells showed a very weak nucleoid staining, and nucleoids were barely visible in most cells. (**B**) PicoGreen staining of a later passage of patient B's fibroblasts also revealed a similar decline in nucleoid staining, compared with earlier passages. (**C**) PicoGreen staining of later passage patient C's fibroblasts. (**D**) Patient D showed occasional depleted fibroblasts. (**E**) There was little difference in PicoGreen staining of early passage (p4) fibroblasts and (**F**) late passage fibroblasts (p25) derived from healthy control. Insets show magnified areas of interest. Bars 20 μm.

disease or from POLG1 patients who were not mosaic for depleted cells (patients G–J). However, in two cell cultures (E and F), occasional depleted cells were apparent (24,25), particularly as the cultures became senescent, but this was not a consistent, progressive feature. Thus the mosaic cellular distribution of mtDNA in fibroblast cultures A–D was characteristic, differing from all other fibroblasts examined and marking them out as a distinctive subgroup.

The mtDNA content of liver was marginally lower in the mosaic patients A–D (average 5%, range 4–7%) than the other patients (average 19%, range 5–32%), but this was not significant ($P = 0.09$). Muscle mtDNA content was also somewhat reduced (average 27%, range 22–32%) but this was not significantly less than the rest of the patients. Muscle mtDNA was normal in the patients with only linker mutations (26), mtDNA content being significantly higher in these than the other patients (average 93 and 34% respectively, $P = 0.001$) with earlier onset Alpers disease (average age 16 and 1 year, respectively, $P < 0.001$).

Characteristics of the cellular mtDNA depletion identified in patients A–C

The reduction in mtDNA content was assessed by quantitative analysis of digital images, which showed that while the number of nucleoids detectable by PicoGreen significantly declined with time (Fig. 2B, $P < 0.001$ and <0.01 for early and late time points for patients B and C, respectively), the distribution of their intensities barely changing (Fig. 2C). That is, nucleoid numbers were reduced (Fig. 2B) but no less intense (Fig. 2C) in depleted cells in the mosaic patients.

We further studied the mosaic mtDNA depletion in cultured cells from patients A–C, using a battery of *in situ* approaches.

Immuno-fluorescence with antibodies against anti-DNA, which detect mtDNA nucleoids as small cytoplasmic dots confirmed the presence of numerous cells within cultures A–C with mosaic and severe mtDNA depletion, which were not

observed in any of the controls (Fig. 3A, top panels). Mitotracker co-labelling indicated many of these depleted cells also exhibited reduced Mitotracker labelling. As Mitotracker specifically labels mitochondria according to their membrane potential, a reduced Mitotracker labelling indicates these mtDNA depleted cells also manifested reduced membrane potential. Similar results were observed with anti-bodies to mitochondrial transcription factor A (TFAM), a nucleoid protein reduced by loss of mtDNA, which showed that numerous cells within cultures A–C exhibited reduced TFAM expression (Fig. 3Af–h), unlike the homogenous labelling of controls (Fig. 3Ae and Supplementary Material, Fig. S1A). Mitotracker co-labelling showed many of the TFAM reduced cells also contained reduced Mitotracker labelling. Interestingly, some mitochondria within anti-DNA/TFAM depleted cells retained Mitotracker labelling, and these invariably co-localized with residual anti-DNA/TFAM expression (arrowed, Fig. 3Ad and Supplementary Material, Fig. S1). Bromodeoxyurudine (BrdU) labelling of newly synthesized DNA within cultures A–C (Fig. 3Aj–l) showed markedly reduced mtDNA replication compared with controls (Fig. 3Ai), with fewer nucleoids incorporating BrdU and a weaker nucleoid labelling. Nuclear BrdU labelling was unaffected. Again, cells with profoundly reduced BrdU also often showed markedly reduced Mitotracker signals (data not shown). A number of patient cells showed a near absence of mtDNA replication (see asterisks in Fig. 3Ak and l).

We next examined the cellular expression of the mtDNA encoded cytochrome *c* oxidase subunit I (COXI, Fig. 3B). COXI immunolabelling showed mosaic COXI expression in cultures A–C, with numerous cells exhibiting reduced COXI, unlike the homogenous expression of controls (Fig. 3Ba–d). Global COXI expression was reduced in cultures A and B (data not shown). COXI reduced cells again often showed substantially reduced Mitotracker labelling, although individual polarized mitochondria often
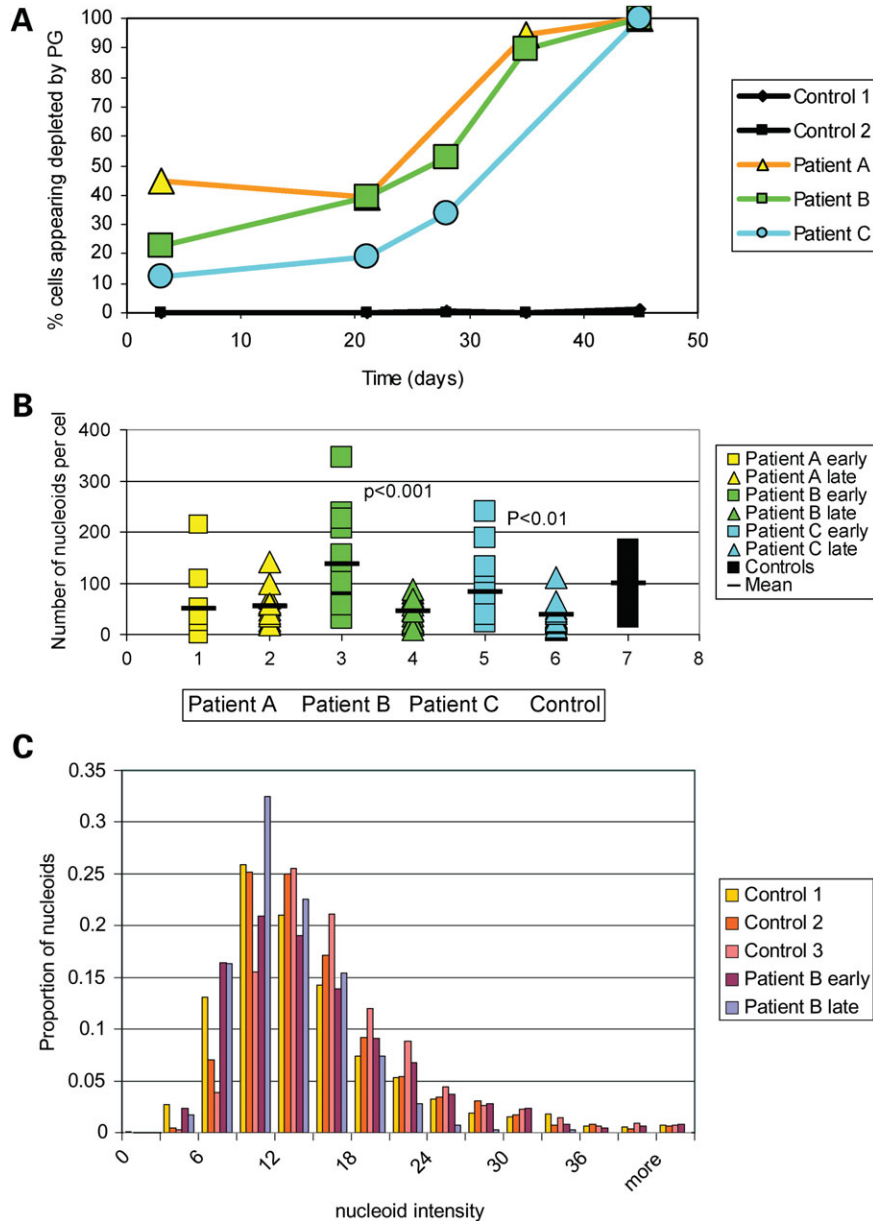
Figure 2. (**A**) Quantification of PicoGreen staining of proportion of mosaic MDS cell cultures A–C that appeared depleted over time. The number of cells that appeared depleted of mtDNA increased over 45 days in the patients but not the controls (200 cells were counted at each time point). Numbers were significantly higher in patients than controls at all time points, other than 28 days ($0.05 < P < 0.0016$). (**B**) Quantification of the numbers of nucleoids visible by PicoGreen staining of mosaic MDS cell cultures A–C and controls [same experiment as (**C**) and Supplementary Material, Fig. S2]. Nucleoid numbers drop with time in MDS cultures ($P < 0.001$ and <0.01 for early and late time points for patients B and C, respectively). In all three patients the number of nucleoids at the late time points are significantly fewer than controls ($P < 0.0002$). (C) Quantification of the intensity of PicoGreen staining of indiviual nucleoids from mosaic MDS cells [same experiment as (B) and Supplementary Material, Fig. S2]. The distribution of nucleoid intensities is similar in patients (early and late passage) and controls (only patient B is shown, whose nucleoid numbers showed the most significant drop).

co-localized with residual COXI expression (arrowed, Supplementary Material, Fig. S3B). A reduced cytochrome *c* oxidase (COX) relative to nuclear encoded succinate dehydrogenase (SDH) activity was detected in many cells within cultures A–C (Fig. 3Be–l).

Finally, to confirm that TFAM, anti-DNA, COXI, BrdU reduced cells within cultures A–D correlated to the PicoGreen reduced cells, we co-labelled these cells with PicoGreen and tetramethyl-rhodamine-methyl ester (TMRM), a dye similar to Mitotracker in that it is absorbed into mitochondria

according to mitochondrial membrane potential (Fig. 3C). Many PicoGreen depleted cells were found to have depolarized mitochondria (Fig. 3C, arrowed).

DISCUSSION

We have found that mtDNA depletion of tissues and cultured fibroblasts from patients with POLG1 mutations is associated particularly with mutations in catalytic domains. We have identified mosaic mtDNA depletion of mtDNA in primary
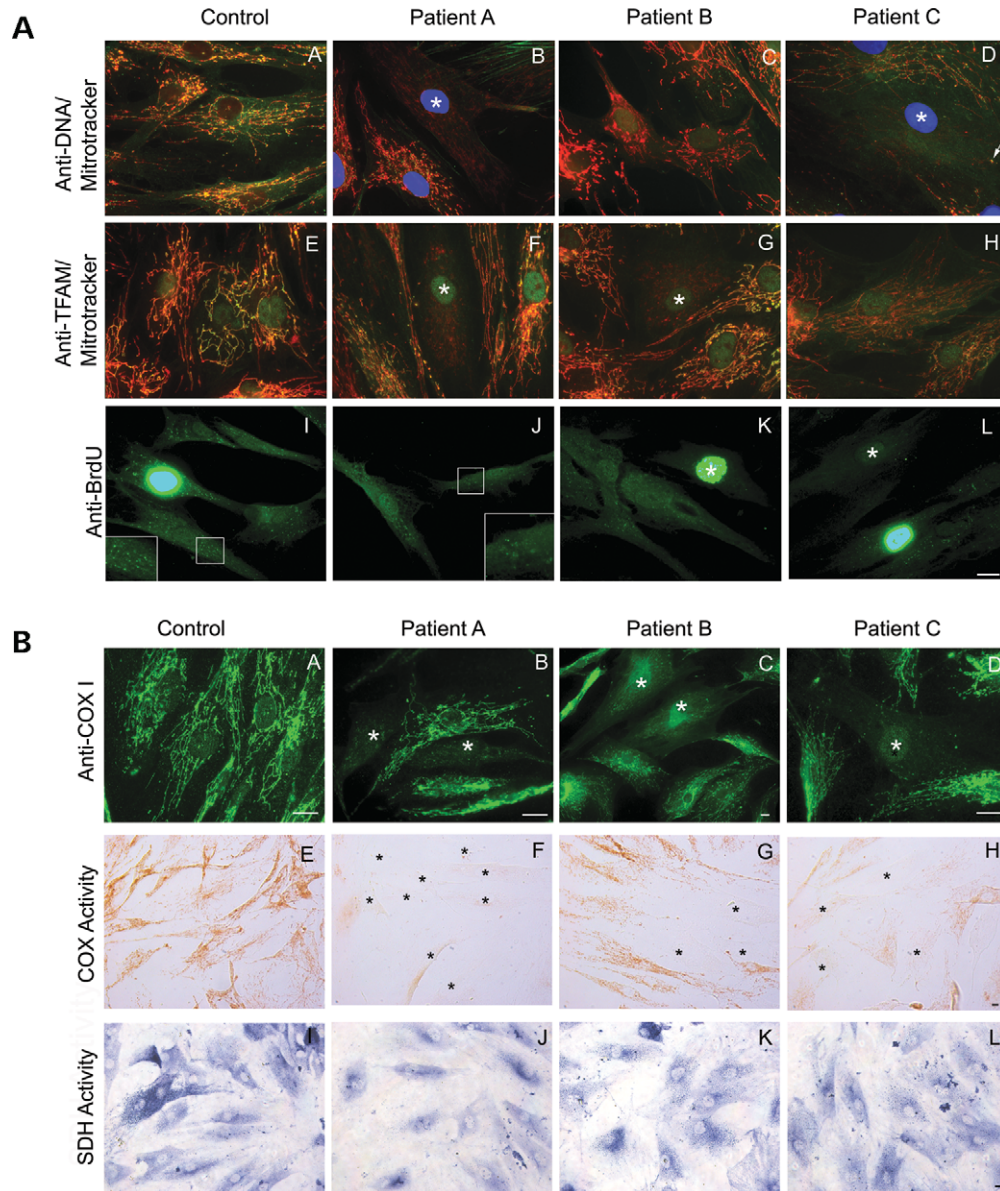
Figure 3. (**A**) MDS cells are mosaic for expression of mtDNA and mitochondrial transcription factor A (TFAM) and have reduced mtDNA synthesis compared with controls. (a) Control fibroblasts co-labelled with anti-DNA antibody (green) and Mitotracker red, showing orange-yellow labelling were there two signals co-localize. (b) Patient A fibroblasts co-labelled with anti-DNA/Mitotracker. (DAPI was used to visualize nuclei blue and an asterisk denotes a cell with no anti-DNA signal). (c) Patient B fibroblasts co-labelled with anti-DNA/Mitotracker. (note: a reduced anti-DNA signal is shown by the predominantly red co-localization with Mitotracker). (d) Patient C fibroblasts co-labelled with anti-DNA/Mitotracker (arrow shows area of residual anti-DNA/mitotracker co-labelling within a depleted cell with reduced Mitotracker labelling). (e) Control fibroblasts co-labelled with anti-TFAM antibody (green) and Mitotracker red. (f) Patient A fibroblasts co-labelled with anti-TFAM/Mitotracker (asterisks show TFAM depleted cells with reduced Mitotracker labelling). (g) Patient B fibroblasts co-labelled with anti-TFAM/Mitotracker. (h) Patient C fibroblasts co-labelled with anti-TFAM/Mitotracker. (i–l) Fibroblasts pulsed with Bromo-deoxyuridine (BrdU) for 220 min, and Br-DNA immuno-detected. (i) BrdU labelling of normal fibroblasts, (j) BrdU labelling of patient A cells (inset shows magnified area of cytoplasm showing weak BrdU labelling). (k) BrdU labelling of patient B cells. (l) BrdU labelling of patient C cells (note: asterisks mark 'ρ° type' cells with very little or no mtDNA labelling). Bar 20 µM. (**B**) Expression of mtDNA encoded cytochrome *c* oxidase subunit I (COXI) in MDS patients is reduced, as is COX activity, but not SDH activity. Cytochrome *c* oxidase subunit I (COXI) expression was monitored using immuno-cytochemistry. (a) COXI labelling of normal control fibroblasts. (b) COXI labelling of patient A fibroblasts (COXI depleted cells are asterisked). (c) COXI labelling of patient B fibroblasts. (d) COXI labelling of patient C fibroblasts. (e–h) Histochemical demonstration of *in situ* COX activity in fibroblasts. (e) COX activity of control. (f) COX activity of patient A cells (asterisks denote cells with markedly reduced activity). (g) COX activity of patient B cells. (h) COX activity of patient C cells. (i–l) Histochemical demonstration of *in situ*SDH activity in fibroblasts. (i) SDH activity of control cells. (j) SDH activity of patient A cells. (k) SDH activity of patient B cells. (l) SDH activity of patient C cells. Bars 20 µM. (**C**) Tetramethyl-rhodamine-methyl ester (TMRM)/PicoGreen co-labelling of mosaic MDS fibroblast mitochondrial membrane potential. (a) PicoGreen labelling of normal control fibroblasts. (b) Co-staining of the same cells with TMRM. (c) Co-localization of the two signals in (a) and (b). (d and e) PicoGreen/TMRM co-labelling of later passage Patient A's fibroblasts. (f) Co-localization of the two signals in (d) and (e). (g and h) PicoGreen/TMRM co-labelling of later passage Patient B's fibroblasts. (i) Co-localization of the two signals. (j and k) PicoGreen/TMRM co-staining of late passage Patient C's cells. (l) Co-localization of the two signals. (m and n) PicoGreen/TMRM co-staining of late passage Patient D's cells. (o) Co-localization of the two signals. Bars 20 µm.
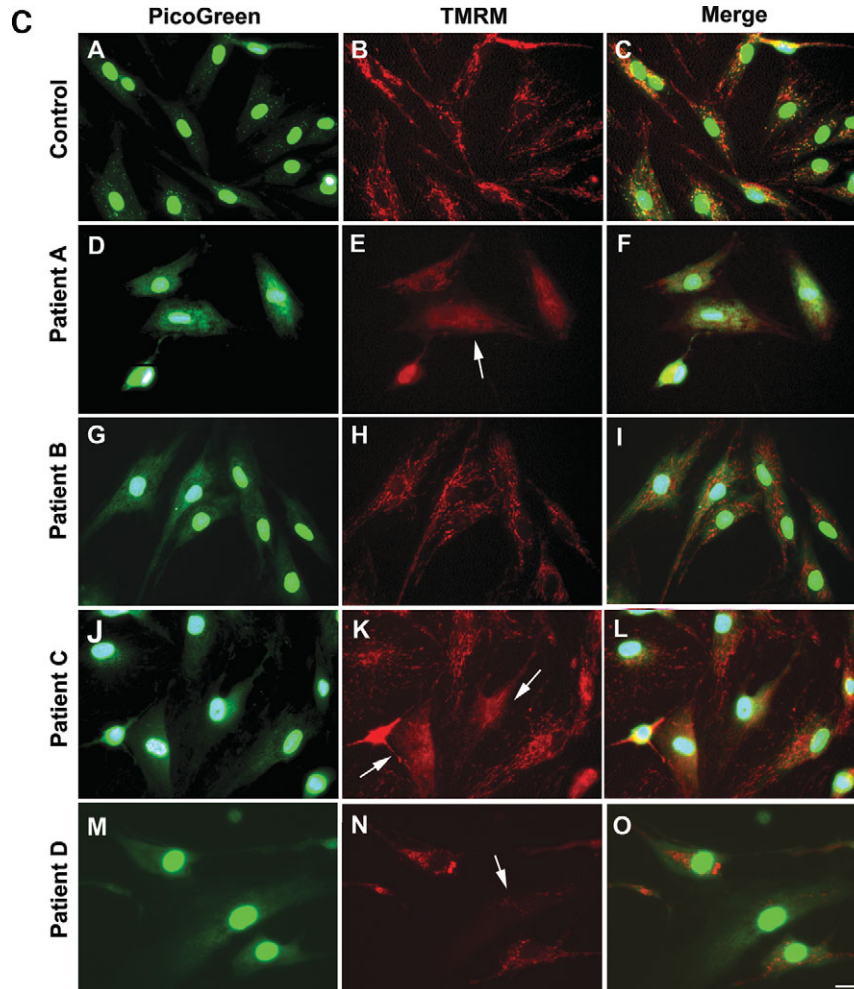
Figure 3. Continued.

fibroblast cultures from some patients with Alpers disease. In patients A–C, mtDNA was depleted in cells with reduced COX activity. These cells also had reduced mitochondrial membrane potential, suggesting that the depletion and not the point mutations underlie the major part of the respiratory chain defect in fibroblasts from these POLG1 patients (Supplementary Material, Fig. S4). In all cases, cellular mosaic depletion was associated with two mutations in catalytic regions of POLG1, either in the polymerase or exonuclease domain or in one of each. The mtDNA depletion manifested primarily as a reduced number of nucleoids in the depleted cells and reflected the severity of the clinical and tissue phenotypes. The cellular mtDNA content may be an indicator of the underlying molecular mechanism that links genotype to phenotype. These data from a human disease suggest that eukaryotic DNA polymerases require both polymerase and $3'-5'$ exonuclease activities within the same molecule.

Previous studies of human POLG1 mutations have found little in the way of clear genotype–phenotype correlations, and these may have been more apparent in the present study as it has been possible to link a range of clinical phenotypes with laboratory data that included both tissue mtDNA content and cellular phenotypes. Our clinical findings were

similar to previous studies, confirming that epilepsy and movement disorders (27) are major features of POLG1 syndromes. Relatively complete information was available for the four patients who manifested mosaic mtDNA depletion, whereas the clinical data available on the other patients was largely retrospective, hence dependent on the local neurologist. We found that the cellular phenotype correlated better with the location of the mutation and the severity of the tissue depletion than with specific clinical features. Nevertheless, mosaic mtDNA depletion was evident in fibroblast cultures from only the most severely affected children, all of whom had died before the age of 16 months. Patient D had two mutations, R232G and T251I, in the exonuclease domain, the latter being in *cis* with the P587L linker mutation. The P587L mutation usually co-segregates with T251I, but has occurred with 251T in a patient with a relatively mild phenotype (28). While this suggests that P587L is mildly pathogenic, T251I may exacerbate its effect. Patient M was homozygous for the L304R exonuclease mutation and had a relatively mild phenotype, but neither liver nor fibroblasts were available for study. In contrast to the patients with two catalytic mutations, no patient who only had missense linker mutations was dead by 16 months or had mosaic cellular or tissue mtDNA depletion.

Table 2. Summary of mutation by location and phenotypic severity: Colour represents severity running from dark orange (most severe) to white (least severe)

Mosaic cellular depletion	Depletion in liver and/or muscle	Location of POLG1 mutation								
		P+P	E+[EL]	E+P	P+L	L+X	E+L	L+L	E+E	Total
Yes	Yes	2	1	1						4
Borderline	Yes				1	1				2
No	Yes				4					4
Unknown	yes				1					1
Unknown	no							2	1	3
unknown	unknown				4	1	2	3		10
	Total	2	1	1	10	2	2	5	1	24

Depletion of mtDNA was present in liver in all cases where it was available for measurement, but was much less consistent than in muscle. All patients with hepatic mtDNA depletion had at least one catalytic mutation, whereas patients with purely linker mutations had little in the way of liver features. These were usually missense mutations, but one patient had a nonsense mutation in the polymerase domain resulting in mono-allelic expression (21,24). We found cellular mtDNA depletion only in individuals with clear tissue depletion (Table 2). The severity of the depletion was commensurate with the severity of the defect in replication that we have seen, and this is supported by the published literature (29). These genotype–phenotype correlations may not have been seen in some previous studies because the diagnosis of mtDNA depletion syndrome is frequently imprecise. This is for both technical reasons (25) and because of the lack of established age-adjusted normal ranges, and may explain some of the inconsistencies in the published literature. However, age-related changes in mtDNA content are undoubtedly also a feature of mtDNA depletion (18,25,30,31). Furthermore, it is clear that the effect of specific mutations may be modulated by other missense mutations in *cis* (32,33).

An important aspect of this study is the use of PicoGreen to visualize mtDNA packaged into nucleoids. While PicoGreen is less sensitive that antiDNA antibodies and does not detect nucleoids containing the lowest levels of mtDNA, it can be used more quantitatively than antiDNA antibodies, being sensitive to the nucleoid DNA content (23). With this method, it could be shown that both the number of nucleoids and the average mtDNA content in individual cells declined with time in fibroblast cultures from the patients with the mosaic cellular depletion phenotype (Fig. 2). During this decline, the distribution of nucleoid intensities remained similar within the range where the PicoGreen signal is quantitative (23). This might indicate that the balance between nucleoid fusion and division depends more on the mtDNA content of the nucleoid than the number of nucleoids in the cell. It may also explain our observation that occasional mitochondria within TFAM depleted cells retained Mitotracker labelling (Supplementary Material, Fig. S2). Occasional nucleoids of relatively normal mtDNA content in cells that are profoundly depleted of mtDNA may underlie the co-localization of Mitotracker and residual TFAM signal.

Like many replicases, POLG1 has a 3′ to 5′ nuclease activity that is used to excise incorrectly paired bases. Mutations in this domain have been seen in both childhood and adult onset POLG1 disease. In the mutator mouse model, POLG1 with deficient exonuclease activity impairs both polymerase fidelity and shortens lifespan (34,−36). By analogy with other DNA polymerases, the enzyme probably alternates between polymerizing and editing modes, as determined by competition between the two active sites for the 3′ primer end of the DNA (37). Once the correct base has been incorporated, the enzyme moves forward 1 bp further, ready for the next precursor nucleotide to enter. Patient B, who is a compound heterozygote with one mutation in the polymerase and one in the exonuclease domain, has a severe cellular and clinical phenotype, comparable with patients A, C and D, who either have two polymerase (patients A and C) or two exonuclease mutations (patient D). The apparent lack of complementation between the POLG1 mutations in patient B supports the molecular model, by suggesting that normal mtDNA replication requires both polymerase and exonuclease activity within the same alpha subunit.

Previous studies of patients with POLG1 mutations have found limited correlation between phenotype and genotype (38–40). Horvath *et al*. (38) reported that patients with Alpers disease generally had at least one catalytic mutation, most commonly in the polymerase domain, and that patients whose mutations both lay in the linker domain presented later. Bindoff and coworkers (27) studied 26 individuals with two common linker mutations, A467T and W748S. The A467T mutation influences the interaction of POLG1 with POLG2 and the W748S mutation reduces both processivity and DNA binding. These authors found major differences in survival depending on genotype, with compound heterozygotes having a significantly shorter survival time than patients homozygous either for the A467T or W748S mutations. As the active form of POLG is known to be a compound heterotrimer containing one alpha and two beta subunits, this suggests a quaternary interaction between catalytic subunits in different heterotrimers. While our data set is much too small to draw parallel inferences, we saw nothing to suggest quaternary interactions between polymerase domains. Patient C, who was homozygous for the R1096C mutation, had a comparable cellular and clinical phenotype to patient A, who was a compound heterozygote for this mutation and T914P.

Six of the other POLG1 mutations we identified have not been reported previously. These comprise one nonsense mutation (R374X), one 10 amino acid deletion (W347_L356del), three simple missense mutations (H277L, R417T, H569Q) and one allele with two missense mutations (P587L;P589L). While P589L is novel, it is in *cis* with P587L which has been reported as a recessive mutation. H277L, R417T and H569Q are all within nine amino acids of previously reported recessive

mutations and alter residues that are highly conserved across mammalian species. In addition, R417T may lead to aberrant splicing as the last nucleotide of exon 6 is mutated (1250G>C).

Wanrooij *et al.* (41) used two dimensional DNA analysis to show that cells, over-expressing POLG1 or TWINKLE containing catalytic defects, have both cellular depletion of mtDNA and replisome stalling. In some of their cell lines, the mtDNA depletion was apparent as reduced numbers of nucleoids. We have previously shown that intra-mitochondrial nucleotide imbalance occurs in cells from patients with mutations in TK2, dGK, TWINKLE and, potentially, TP (24). Nucleotide imbalance is another potential cause of replisome pausing and depletion, and cells that are deficient in dGK may also have mosaic mtDNA depletion (25,42). Replisome pausing may thus underlie mtDNA depletion due to either POLG1 mutations (41) or to nucleotide imbalances (43). The mosaic cellular depletion that we have demonstrated may thus be a manifestation of severe replication stalling. As in the model proposed by Wanrooij *et al.*, we found that each of the fibroblast cultures from patients A–D (that had the most severe cellular depletion) had at least two POLG1 mutations lying in catalytic domains. The depletion in the patient cells was less pronounced than in the *in vitro* study, however, the progressive depletion observed with successive passages of patient cells may partly recapitulate the depletion observed on induction of the mutant POLG1 in the experimental study.

The clinical findings in this group of patients are similar to those found in previous studies of POLG1 mutations in Alpers disease. The prominence of epilepsy has been highlighted before, as well as the variability in pointers to mitochondrial disease. Movement disorders appear to be very much more common than in maternally inherited mtDNA disease, especially if this feature is broadened to include epilepsia partialis continua. Thus, epilepsia partialis continua and movement disorders may provide an important pointer to POLG1 mutations. In one case, fatal deterioration followed valproate therapy and others have reported a clear improvement on stopping therapy with this anticonvulsant. However, several other patients, with a generally milder phenotype, have been treated with this drug for short periods without apparent problem. The relationship between the hepatic encephalopathy associated with valproate therapy and pre-existing POLG mutations (carrier frequency <1 in 150) is worthy of further study.

Among a group of patients with POLG1 mutations, we have identified and characterized mosaic cellular depletion of mitochondrial DNA in four patients, each with two mutations affecting catalytic domains. These mutations appear to have severe consequences, both for the clinical phenotype and the mtDNA content of affected tissues. Patients with demonstrable tissue mtDNA depletion always had at least one catalytic domain or nonsense mutation. Our findings add general support to the current model of the role of POLG1 in the replisome.

MATERIALS AND METHODS

Patients

Patients were referred to our diagnostic service with a variety of clinical presentations. In two cases (we received fibroblasts, the patients having been diagnosed at other centres [patient D

(37) and J (21,24)]. Alpers was diagnosed on the basis of the referring clinician's information, some of which was collected retrospectively (Table 1). Case histories for patients A–C are in the Supplementary Material.

Materials

All chemicals were from Sigma-Aldrich Ltd or Biomol International. Antibodies to TFAM were raised in our own lab, anti-DNA was from ProGen Biotechnick GmbH. Anti-BrdU antibody was from Roche. Alexafluor secondary antibodies, mouse anti-COXI, PicoGreen and Mitotracker Red were from Invitrogen Corp.

Cell culture

Fibroblast cultures were all free of mycoplasma by routine screening and were cultured in Dulbeco's modified essential medium, with 4.5 g/l glucose supplemented with 10% fetal bovine serum (PCL International UK Ltd), 20 mM pyruvate, 2 mM glutamate and 100 units/ml penicillin/streptomycin and 50 μM uridine.

DNA extraction

Approximately 4×10^6 cells were re-suspended in 2 ml of DNA extraction buffer and incubated at 50°C for 1–3 h. The DNA was then precipitated with the addition of an equal volume of isopropanol at room temperature and the DNA pellet washed three times in 70% ethanol before air drying, and re-suspension Tris–EDTA buffer, pH 7.4. In some experiments DNA was extracted by using a QIAamp DNA mini kit, as per manufacturer's instructions.

Cytochemical staining

Cells were grown overnight in six well plates. MtDNA staining in live cells was achieved by diluting stock PicoGreen solution at 3 μl/ml (1–3 h). The cells were rinsed three times in pre-warmed PBS and mounted with phenol red free DMEM supplemented with 4.5 g/l glucose and 25 mM HEPES buffer, and visualized using an epifluorescent microscope. Cells were co-stained after PicoGreen labelling with TMRM by incubation for 30 min in medium containing 30 nM TMRM at 37°C.

For immunocytochemical staining, cells were fixed for 20 min with 4% paraformaldehyde in PBS, and permeabilized with 0.5% triton-X in PBS for 15 min. The cells were then incubated with primary antibodies for 1 h. Antibody dilutions were anti-TFAM antibody at 1:60, anti-COX subunit I at 10 μg/ml, anti-DNA 1:10. After incubation, the cells were rinsed in PBS and primary antibodies were visualized using fluorescent-tagged secondary antibodies. Antibody dilutions were: Anti-rabbit FITC (1:60), anti-mouse FITC (1:75), anti-rabbit TRITC (1:60). After incubation, the cells were counterstained with 0.5 μg/ml DAPI, rinsed in PBS X3, and mounted using Hydromount. For Mitotracker co-labelling cells were incubating with 100 nM Mitotracker for 30 min, with a further 25 min in dye-free medium, before fixation.

For bromodeoxyuridine labelling of newly synthesized DNA (44), cells were incubated for 3–7 h in DMEM supplemented with 15 μM bromodeoxyuridine (BrdU), and fixed in glycine fix (−20°C) for 40 min. The cells were gently re-hydrated and the cells were incubated with anti-BrdU with nucleases, for 45 min at 37°C. The primary was visualized with an anti-mouse secondary, and the cells mounted.

Histochemical staining of cytochrome *c* oxidase and SDH activity

Cells to be stained for cytochrome *c* oxidase (COX) activity were grown on sterile glass cover slips overnight. Cells were rinsed with ice-cold PBS, and once with 50% PBS in water, and all traces of fluid removed. Cells were air-dried and then incubated at 37°C with freshly prepared modified staining buffer, consisting of 10% sucrose, 100 μM of fully reduced bovine cytochrome *c*, 8 units catalase, 1 mg/ml DAB and 0.25% DMSO, 10% sucrose in 20 mM sodium phosphate buffer (pH 7). After incubations, a brown deposit of insoluble DAB polymer representing COX activity is generated by single electron reduction of DAB monomer. The staining buffer was removed, and the cells rinsed once with 20 mM phosphate buffer, followed by post fixation in 4% paraformaldehyde, and mounted in Hydromount. An azide treated negative control was included with each experiment.

SDH activity was measured as described (45), with modifications. The cells were air-dried as above, and incubated in 0.1M phosphate buffer (pH 7) containing 1.5 mM nitroblue tetrazolium, 130 mM sodium succinate, 0.2 mM phenazine methosulfate and 1.0 mM sodium azide, for 1–2 h at 37°C.

Microscopy and digital image analysis. Image capture was done using SimplePCI, and figures were constructed with Photoshop. Quantitative image analysis was performed on unprocessed images using ImageJ (http://rsb.info.nih.gov/ij/download.html), and fluorescent intensities calculated using the sum of pixel grey scale values, corrected for mean local cellular background.

Real-time quantitative PCR. Estimation of relative mtDNA to nDNA levels were performed as described previously (23), except the nuclear probe was labelled with Vic at the 5′ end and the amplification reactions were done simultaneously using a GeneAmp 7700 sequence detection system.

Statistical analysis

t-tests were carried out using the SPSS package version 15.0.

Analysis of the POLG gene

The entire coding region and flanking intronic regions (at least 10 nucleotides) of *POLG* were amplified by PCR from genomic DNA and sequenced by fluorescent dideoxy sequencing (Applied Biosystems BigDye Terminator v1.1 kit) and capillary electrophoresis (Applied Biosystems 3730) (primers and conditions available on request). Results were compared with GenBank reference sequences NT_033276.4 and NM_002693.1. Nucleotide numbering was assigned using the A of the ATG translation initiation codon as nucleotide 1. The *POLG* p.A467T, p.W748S and p.G848S mutations were also analysed by PCR and restriction enzyme digest (primers, restriction enzymes and conditions available on request).

SUPPLEMENTARY MATERIAL

Supplementary Material is available at HMG Online.

REFERENCES

1. Moraes, C.T., Shanske, S., Tritschler, H.J., Aprille, J.R., Andreetta, F., Bonilla, E., Schon, E.A. and DiMauro, S. (1991) mtDNA depletion with variable tissue expression: a novel genetic abnormality in mitochondrial diseases. *Am. J. Hum. Genet.*, **48**, 492–501.
2. Moraes, C., Ricci, E., Arnaudo, E., Bonilla, E., DiMauro, S. and Schon, E. (1993) Quantitative defects of mitochondrial DNA. In DiMauro, S. and Wallace, D. (eds), *Mitochondrial DNA in Human Pathology*. Raven, New York, pp. 97–108.
3. Barthelemy, C., de Baulny, H.O. and Lombes, A. (2002) D-loop mutations in mitochondrial DNA: link with mitochondrial DNA depletion? *Hum. Genet.*, **110**, 479–487.
4. Taanman, J.W., Bodnar, A.G., Cooper, J.M., Morris, A.A., Clayton, P.T., Leonard, J.V. and Schapira, A.H. (1997) Molecular mechanisms in mitochondrial DNA depletion syndrome. *Hum. Mol. Genet.*, **6**, 935–942.
5. Blake, J.C., Taanman, J.W., Morris, A.M., Gray, R.G., Cooper, J.M., McKiernan, P.J., Leonard, J.V. and Schapira, A.H. (1999) Mitochondrial DNA depletion syndrome is expressed in amniotic fluid cell cultures. *Am. J. Pathol.*, **155**, 67–70.
6. Bodnar, A.G., Cooper, J.M., Holt, I.J., Leonard, J.V. and Schapira, A.H. (1993) Nuclear complementation restores mtDNA levels in cultured cells from a patient with mtDNA depletion. *Am. J. Hum. Genet.*, **53**, 663–669.
7. Saada, A., Shaag, A. and Elpeleg, O. (2003) mtDNA depletion myopathy: elucidation of the tissue specificity in the mitochondrial thymidine kinase (TK2) deficiency. *Mol. Genet. Metab.*, **79**, 1–5.
8. Spinazzola, A. and Zeviani, M. (2005) Disorders of nuclear-mitochondrial intergenomic signaling. *Gene*, **354**, 162–168.
9. Suomalainen, A. and Kaukonen, J. (2001) Diseases caused by nuclear genes affecting mtDNA stability. *Am. J. Med. Genet.*, **106**, 53–61.
10. Naviaux, R.K. and Nguyen, K.V. (2004) POLG mutations associated with Alpers' syndrome and mitochondrial DNA depletion. *Ann. Neurol.*, **55**, 706–712.
11. Mandel, H., Szargel, R., Labay, V., Elpeleg, O., Saada, A., Shalata, A., Anbinder, Y., Berkowitz, D., Hartman, C., Barak, M. *et al.* (2001) The deoxyguanosine kinase gene is mutated in individuals with depleted hepatocerebral mitochondrial DNA. *Nat. Genet.*, **29**, 337–341.
12. Spinazzola, A., Viscomi, C., Fernandez-Vizarra, E., Carrara, F., D'Adamo, P., Calvo, S., Marsano, R.M., Donnini, C., Weiher, H., Strisciuglio, P. *et al.* (2006) MPV17 encodes an inner mitochondrial membrane protein and is mutated in infantile hepatic mitochondrial DNA depletion. *Nat. Genet.*, **38**, 570–575.

13. Hakonen, A.H., Isohanni, P., Paetau, A., Herva, R., Suomalainen, A. and Lonnqvist, T. (2007) Recessive Twinkle mutations in early onset encephalopathy with mtDNA depletion. *Brain*, **130**, 3032–3040.

14. Ostergaard, E., Christensen, E., Kristensen, E., Mogensen, B., Duno, M., Shoubridge, E.A. and Wibrand, F. (2007) Deficiency of the alpha subunit of succinate-coenzyme A ligase causes fatal infantile lactic acidosis with mitochondrial DNA depletion. *Am. J. Hum. Genet.*, **81**, 383–387.

15. Elpeleg, O., Miller, C., Hershkovitz, E., Bitner-Glindzicz, M., Bondi-Rubinstein, G., Rahman, S., Pagnamenta, A., Eshhar, S. and Saada, A. (2005) Deficiency of the ADP-Forming succinyl-CoA synthase activity is associated with encephalomyopathy and mitochondrial DNA depletion. *Am. J. Hum. Genet.*, **76**, 1081–1086.

16. Bourdon, A., Minai, L., Serre, V., Jais, J.P., Sarzi, E., Aubert, S., Chretien, D., de Lonlay, P., Paquis-Flucklinger, V., Arakawa, H. *et al.* (2007) Mutation of RRM2B, encoding p53-controlled ribonucleotide reductase (p53R2), causes severe mitochondrial DNA depletion. *Nat. Genet.*, **39**, 776–780.

17. Nishino, I., Spinazzola, A. and Hirano, M. (1999) Thymidine phosphorylase gene mutations in MNGIE, a human mitochondrial disorder. *Science*, **283**, 689–692.

18. Barthelemy, C., Ogier de Baulny, H., Diaz, J., Cheval, M.A., Frachon, P., Romero, N., Goutieres, F., Fardeau, M. and Lombes, A. (2001) Late-onset mitochondrial DNA depletion: DNA copy number, multiple deletions, and compensation. *Ann. Neurol.*, **49**, 607–617.

19. Chinnery, P.F. and Zeviani, M. (2007) 155th ENMC workshop: Polymerase gamma and disorders of mitochondrial DNA synthesis, 21–23 September 2007, Naarden, The Netherlands. *Neuromuscul. Disord.*, **18**, 259–267.

20. Hakonen, A.H., Heiskanen, S., Juvonen, V., Lappalainen, I., Luoma, P.T., Rantamaki, M., Goethem, G.V., Lofgren, A., Hackman, P., Paetau, A. *et al.* (2005) Mitochondrial DNA polymerase W748S mutation: a common cause of autosomal recessive ataxia with ancient European origin. *Am. J. Hum. Genet.*, **77**, 430–441.

21. Chan, S.S., Longley, M.J., Naviaux, R.K. and Copeland, W.C. (2005) Mono-allelic POLG expression resulting from nonsense-mediated decay and alternative splicing in a patient with Alpers syndrome. *DNA Repair (Amst)*, **4**, 1381–1389.

22. Harding, B.N., Alsanjari, N., Smith, S.J., Wiles, C.M., Thrush, D., Miller, D.H., Scaravilli, F. and Harding, A.E. (1995) Progressive neuronal degeneration of childhood with liver disease (Alpers' disease) presenting in young adults. *J. Neurol. Neurosurg. Psychiatry*, **58**, 320–325.

23. Ashley, N., Harris, D. and Poulton, J. (2005) Detection of mitochondrial DNA depletion in living human cells using PicoGreen staining. *Exp. Cell Res.*, **303**, 432–446.

24. Ashley, N., Adams, S., Slama, A., Zeviani, M., Suomalainen, A., Andreu, A., Naviaux, R. and Poulton, J. (2007) Defects in maintenance of mitochondrial DNA are associated with intramitochondrial nucleotide imbalances. *Hum. Mol. Genet.*, **16**, 1400–1411.

25. Morten, K.J., Ashley, N., Wijburg, F., Hadzic, N., Parr, J., Jayawant, S., Adams, S., Bindoff, L., Bakker, H.D., Mieli-Vergani, G. *et al.* (2007) Liver mtDNA content increases during development: a comparison of methods and the importance of age- and tissue-specific controls for the diagnosis of mtDNA depletion. *Mitochondrion*, **16**, 1400–1411.

26. Van Goethem, G., Luoma, P., Rantamaki, M., Al Memar, A., Kaakkola, S., Hackman, P., Krahe, R., Lofgren, A., Martin, J.J., De Jonghe, P. *et al.* (2004) POLG mutations in neurodegenerative disorders with ataxia but no muscle involvement. *Neurology*, **63**, 1251–1257.

27. Tzoulis, C., Engelsen, B.A., Telstad, W., Aasly, J., Zeviani, M., Winterthun, S., Ferrari, G., Aarseth, J.H. and Bindoff, L.A. (2006) The spectrum of clinical disease caused by the A467T and W748S POLG mutations: a study of 26 cases. *Brain*, **129**, 1685–1692.

28. Gonzalez-Vioque, E., Blazquez, A., Fernandez-Moreira, D., Bornstein, B., Bautista, J., Arpa, J., Navarro, C., Campos, Y., Fernandez-Moreno, M.A., Garesse, R. *et al.* (2006) Association of novel POLG mutations and multiple mitochondrial DNA deletions with variable clinical phenotypes in a Spanish population. *Arch. Neurol.*, **63**, 107–111.

29. Stuart, G.R., Santos, J.H., Strand, M.K., Van Houten, B. and Copeland, W.C. (2006) Mitochondrial and nuclear DNA defects in *Saccharomyces cerevisiae* with mutations in DNA polymerase {gamma} associated with progressive external ophthalmoplegia. *Hum. Mol. Genet.*, **15**, 363–374.

30. Vila, M.R., Segovia-Silvestre, T., Gamez, J., Marina, A., Naini, A.B., Meseguer, A., Lombes, A., Bonilla, E., DiMauro, S., Hirano, M. *et al.* (2003) Reversion of mtDNA depletion in a patient with TK2 deficiency. *Neurology*, **60**, 1203–1205.

31. Ducluzeau, P.H., Lachaux, A., Bouvier, R., Duborjal, H., Stepien, G., Bozon, D. and Mousson de Camaret, B. (2002) Progressive reversion of clinical and molecular phenotype in a child with liver mitochondrial DNA depletion. *J. Hepatol.*, **36**, 698–703.

32. Chan, S.S., Longley, M.J. and Copeland, W.C. (2006) Modulation of the W748S mutation in DNA polymerase {gamma} by the E1143G polymorphism in mitochondrial disorders. *Hum. Mol. Genet.*, **15**, 3473–3483.

33. Hudson, G. and Chinnery, P.F. (2006) Mitochondrial DNA polymerase-gamma and human disease. *Hum. Mol. Genet.*, **15** (Spec no. 2), R244–R252.

34. Trifunovic, A., Wredenberg, A., Falkenberg, M., Spelbrink, J.N., Rovio, A.T., Bruder, C.E., Bohlooly, Y.M., Gidlof, S., Oldfors, A., Wibom, R. *et al.* (2004) Premature ageing in mice expressing defective mitochondrial DNA polymerase. *Nature*, **429**, 417–423.

35. Graziewicz, M.A., Bienstock, R.J. and Copeland, W.C. (2007) The DNA polymerase gamma Y955C disease variant associated with PEO and parkinsonism mediates the incorporation and translesion synthesis opposite 7,8-dihydro-8-oxo-2'-deoxyguanosine. *Hum. Mol. Genet.*, **16**, 2729–2739.

36. Trifunovic, A., Hansson, A., Wredenberg, A., Rovio, A.T., Dufour, E., Khvorostov, I., Spelbrink, J.N., Wibom, R., Jacobs, H.T. and Larsson, N.G. (2005) Somatic mtDNA mutations cause aging phenotypes without affecting reactive oxygen species production. *Proc. Natl Acad. Sci. USA*, **102**, 17993–17998.

37. Lewin, B. (2004) DNA replication. In G, Carson. (ed), *Genes VIII*, Pearson Education International, pp. 387–392.

38. Horvath, R., Hudson, G., Ferrari, G., Futterer, N., Ahola, S., Lamantea, E., Prokisch, H., Lochmuller, H., McFarland, R., Ramesh, V. *et al.* (2006) Phenotypic spectrum associated with mutations of the mitochondrial polymerase gamma gene. *Brain*, **129**, 1674–1684.

39. Ferrari, G., Lamantea, E., Donati, A., Filosto, M., Briem, E., Carrara, F., Parini, R., Simonati, A., Santer, R. and Zeviani, M. (2005) Infantile hepatocerebral syndromes associated with mutations in the mitochondrial DNA polymerase-gammaA. *Brain*, **128**, 723–731.

40. Alberio, S., Mineri, R., Tiranti, V. and Zeviani, M. (2007) Depletion of mtDNA: syndromes and genes. *Mitochondrion*, **7**, 6–12.

41. Wanrooij, S., Goffart, S., Pohjoismaki, J.L., Yasukawa, T. and Spelbrink, J.N. (2007) Expression of catalytic mutants of the mtDNA helicase Twinkle and polymerase POLG causes distinct replication stalling phenotypes. *Nucleic Acids Res.*, **35**, 3238–3251.

42. Taanman, J.W., Muddle, J.R. and Muntau, A.C. (2003) Mitochondrial DNA depletion can be prevented by dGMP and dAMP supplementation in a resting culture of deoxyguanosine kinase-deficient fibroblasts. *Hum. Mol. Genet.*, **12**, 1839–1845.

43. Baruffini, E., Lodi, T., Dallabona, C., Puglisi, A., Zeviani, M. and Ferrero, I. (2006) Genetic and chemical rescue of the *Saccharomyces cerevisiae* phenotype induced by mitochondrial DNA polymerase mutations associated with progressive external ophthalmoplegia in humans. *Hum. Mol. Genet.*, **15**, 2846–2855.

44. Magnusson, J., Orth, M., Lestienne, P. and Taanman, J.W. (2003) Replication of mitochondrial DNA occurs throughout the mitochondria of cultured human cells. *Exp. Cell Res.*, **289**, 133–142.

45. Elson, J.L., Samuels, D.C., Johnson, M.A., Turnbull, D.M. and Chinnery, P.F. (2002) The length of cytochrome c oxidase-negative segments in muscle fibres in patients with mtDNA myopathy. *Neuromuscul. Disord.*, **12**, 858–864.